DOI: https://doi.org/10.37434/tpwj2024.05.01

PECULIARITIES OF FRACTURE OF WELDED JOINTS OF RAILWAY RAILS OF OXYGEN-CONVERTER K76F STEEL

V.I. Shvets, I.V. Ziakhor, L.M. Kapitanchuk, O.V. Didkovskyi, E.V. Antipin

E.O. Paton Electric Welding Institute of the NASU
11 Kazymyr Malevych Str., 03150, Kyiv, Ukraine

ABSTRACT

The fracture surface of rail K76F steel after static bending tests of rail butt joints produced by flash-butt welding was studied. Butt joints of rails of individual batches were fractured on the base metal or heat-affected zone (HAZ). It is shown that in the regions of dark colour and oval shape, the fracture on the iron oxide film takes place. The formation of films occurs as a result of melting and distribution of iron oxide inclusions along the structural boundaries probably in the thermo-deformation conditions of the crimping shop at the stage of blooming production. The formation of clusters of iron oxides occurs during the crystallization of the residual melt in steel ingots with an insufficient degree of deoxidation. Oval regions of dark colour on the fracture surface are evidence of an insufficient degree of deoxidation of rail steel and a factor of its quality reduction.

KEYWORDS: rail K76F steel, deoxidation, flash-butt welding, iron oxide

INTRODUCTION

At present, the oxygen-converter method is mainly used for melting rail steel. Compared to the open-hearth method, it is distinguished by higher efficiency, lower capital costs, more favourable conditions for mechanization and automation of production processes, combination of the process of steel melting with continuous casting. The essence of the oxygen-converter method consists in blowing of liquid pig iron with oxygen in the aggregate-converter. Under the action of oxygen, pig iron impurities like manganese, silicon and, above all, carbon are oxidized and removed from the melt.

JSC Ukrzaliznytsia uses R65 type rails of K76F grade of converter production, hardened with induction heating along the entire length of rolling surface and side edges [1]. The results of qualification tests showed that the developed technology of rail production provided the compliance of their properties with the requirements of regulatory documents [2]. To join rails during the construction of railway tracks, the technology of flash-butt welding was used, developed at the PWI of the NASU and successfully realized in practice [3, 4].

During mechanical static bending tests, fracturing of rail joints usually occurs on the butt joint. The rail joints of individual batches were fractured on the base metal or HAZ. During visual inspection, regions of the oval shape were detected on the fracture surface, which were of dark colour due to peculiar features of the relief. In the work, these regions are defined as "oval spots" (OS) (Figure 1). OS, which were nuclei of butt joint fracture, were located mainly in the rail head (Figure 1, *a*), rarely — in the foot (Figure 1, *b*).

The aim of the work consisted in finding the nature and causes of OS formation on the fracture surface of welded butt joints of K76F rails.

PROCEDURE AND EQUIPMENT

K76F rails were investigated after fracturing of butt joints during the static bending tests. Analysis of the rail macrostructure was carried out on templates

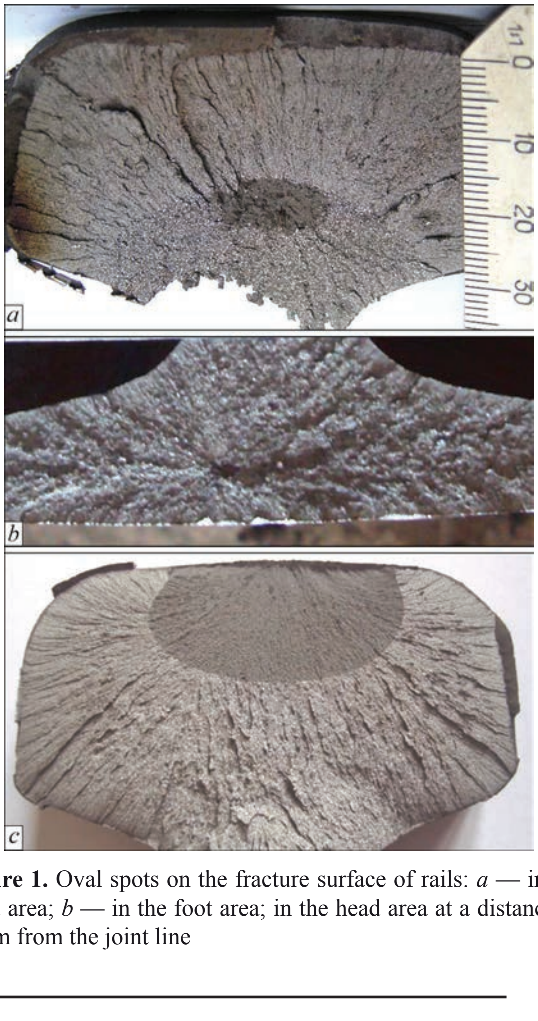

Figure 1. Oval spots on the fracture surface of rails: *a* — in the head area; *b* — in the foot area; in the head area at a distance of 7 mm from the joint line

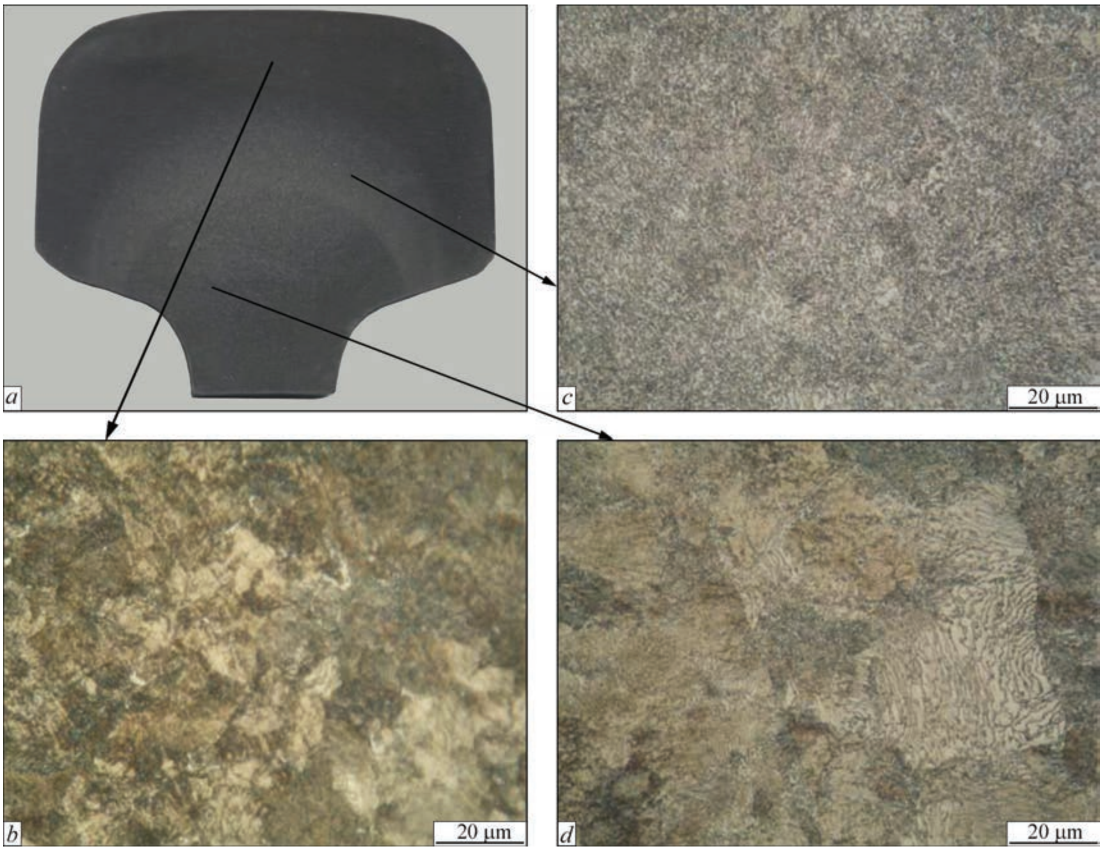

Figure 2. *a* — rail macrostructure in the head area, ×1000; *b* — near-surface layer; *c* — tempering regions; *d* — base metal

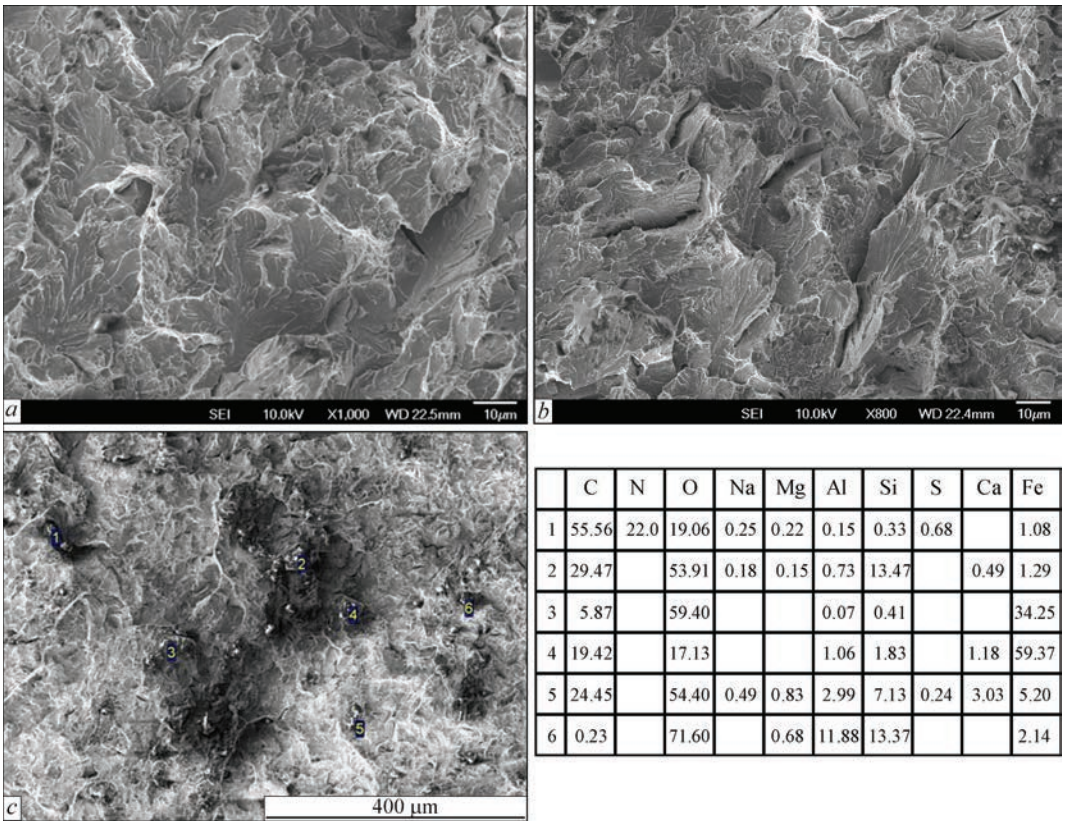

	C	N	O	Na	Mg	Al	Si	S	Ca	Fe
1	55.56	22.0	19.06	0.25	0.22	0.15	0.33	0.68		1.08
2	29.47		53.91	0.18	0.15	0.73	13.47		0.49	1.29
3	5.87		59.40			0.07	0.41			34.25
4	19.42		17.13			1.06	1.83		1.18	59.37
5	24.45		54.40	0.49	0.83	2.99	7.13	0.24	3.03	5.20
6	0.23		71.60		0.68	11.88	13.37			2.14

Figure 3. Fracture surface in the region of heat-hardened layer (*a*, *b*), nonmetallic inclusions (*c*) and results of X-ray microanalysis of chemical composition (at.%)

Table 1. Chemical composition of K76F rails, wt.%

Element	C	Mn	Si	V	Ti	Cr	P	Al	S
Grade composition	0.71–0.82	0.80–1.30	0.25–0.45	0.03–0.07	–	≤0.15	≤0.035	≤0.015	≤0.04
Composition of investigated rails	0.76	0.85	0.317	<0.02	0.005	0.04	0.013	0.015	<0.03

cut out in the cross direction. Microstructure examinations were conducted in the optical microscope NEOPHOT-32, equipped with a digital camera. Microstructure was revealed by etching of preliminary polished specimens in a 4 % HNO_3 alcohol solution. To analyze the microstructure and chemical heterogeneity of the fracture surface during fracturing on the base metal, Auger-microprobe JAMP 9500F of JEOL Company (Japan) was used, on which the X-ray energy dispersive spectrometer JNCA Penta FET x3 of Oxford Instrument Company is installed. The energy of the primary electron beam was 10 keV at a current of 0.5 nA for the method of micro X-ray diffraction analysis (MXRD) and of 10 nA for the method of Auger-electron spectroscopy. To build the distribution of elements in depth, the specimen surface was bombarded by Ar^+ ions (ion etching) with the energy of 3 keV and etching rate of 20 nm/min. Vickers's hardness was measured in a hardness tester NOVOTEST TC-GPB with a load of 292.4 N (30 kg).

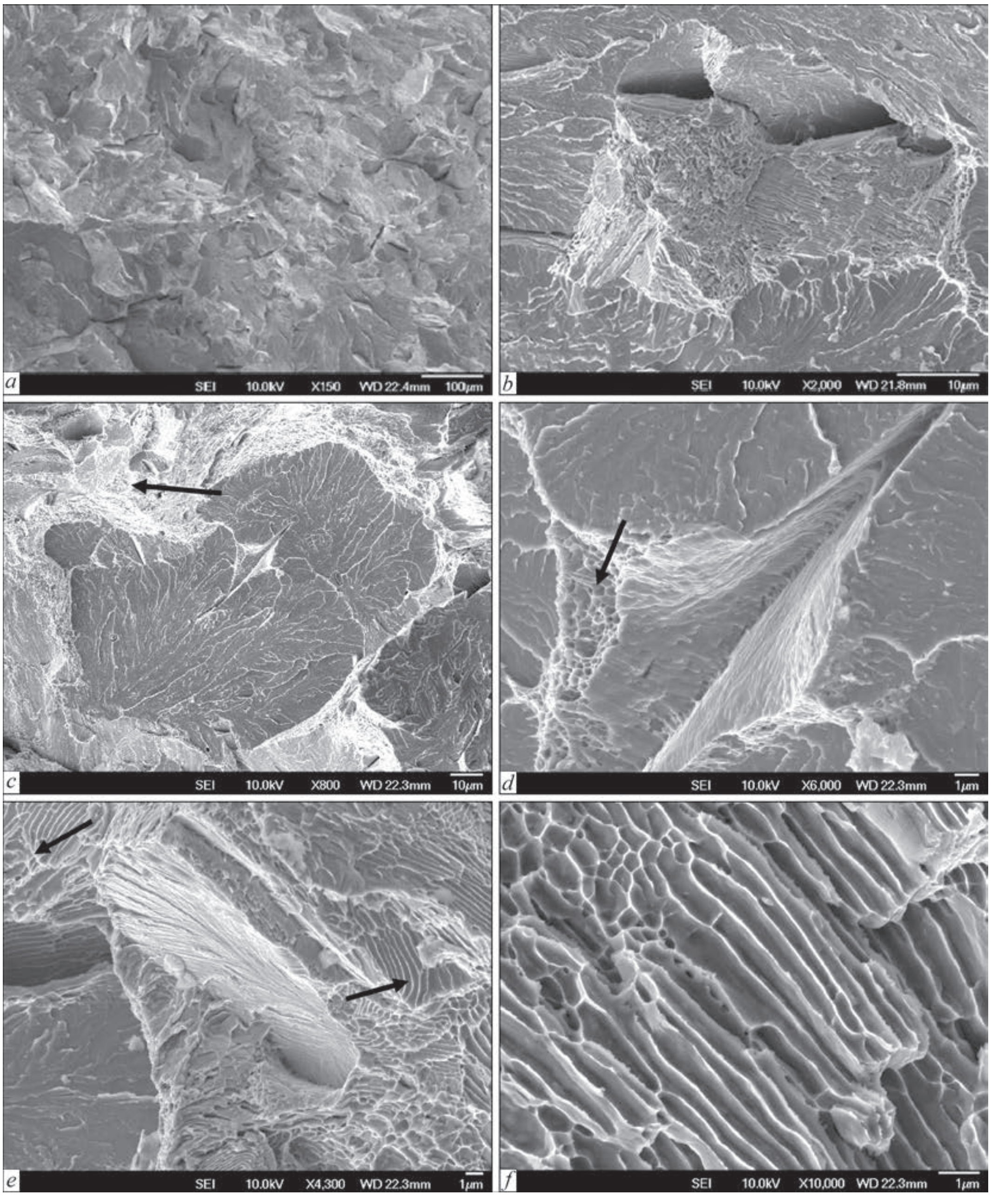

Figure 4. Fracture surface in the tempering region (*a*, *b*); opening of metal on the film of iron oxide (*c*, *d*); opening of metal on the pearlite colonies (*e*, *f*)

RESEARCH RESULTS AND DISCUSSION

According to the results of spectral analysis, the chemical composition of the metal in the investigated rails corresponds to the grade one (Table 1). The rail macrostructure does not reveal disorders of metal continuity. In the head area, the regions of HAZ are clearly revealed, typical for the rails after surface heat treatment (Figure 2, *a*). Near the rolling surface, a heat-hardened layer of dark colour of up to 15 mm width is observed. This layer is adjacent to a layer of gray colour (tempering area), which is distinguished by a reduced hardness compared to the near-surface layer and base metal: *HV* 2430–2680 MPa, *HV* 3590–3800 MPa and *HV* 2700–3040 MPa, respectively. Microstructure of the near-surface layer of a dark colour is sorbite (Figure 2, *b*), and that of a gray layer and the base metal is sorbite-pearlite (Figure 2, *c*, *d*).

Fractographic examinations of the fracture surface during fracturing on the base metal showed that within the heat-hardened layer, the fracture is transcrystalline. The fracture surface consists of facets of intragranular spalling with elements of plastic deformation: stream-like pattern, tongues, tear crests (Figure 3, *a*). In some places, secondary cracks are encountered (Figure 3, *b*). Nonmetallic inclusions on the fracture surface are represented by complex oxides of aluminium, calcium and silicon (Figure 3, *c*; Table 1). The formation of oxide clusters is a cause for the formation of a developed relief in this region.

In the tempering region, the fracture is mostly transcrystalline. However, fracturing is accompanied by the formation of spalling facets (Figure 4, *a*). Numerous secondary cracks (Figure 4, *b*) are present near spalling facets in the microstructure, places of metal opening on the film structural component (Figure 4, *c*, *d*) and pearlite colonies (Figure 4, *d*, *e*) are observed.

In the OS region, unlike in the tempering regions and a heat-hardened layer, the fracture is intercrystalline (Figure 5, *a*). The fracturing surface is dimple (Figure 5, *b*). According to the chemical composition, the particles, which are located in the dimples and determine the nature of fracture, are iron oxide (Figure 5, *c*, Table 1). The size of the particles is the tenth fractions of a micron.

Using the method of Auger-electronic spectroscopy, the elemental composition and its changes during layer-by-layer ion etching of the dimple surface were analyzed. Figure 6 shows the place of shooting, spectra before and after ion etching, as well as a table with the content of elements calculated by spectra. As is seen, the surface layer contains iron, oxygen and a small amount of aluminium. According to the profile of the element distribution in depth, the width of the layer with the elemental composition different from the base metal was about 50 A (Figure 7). The results

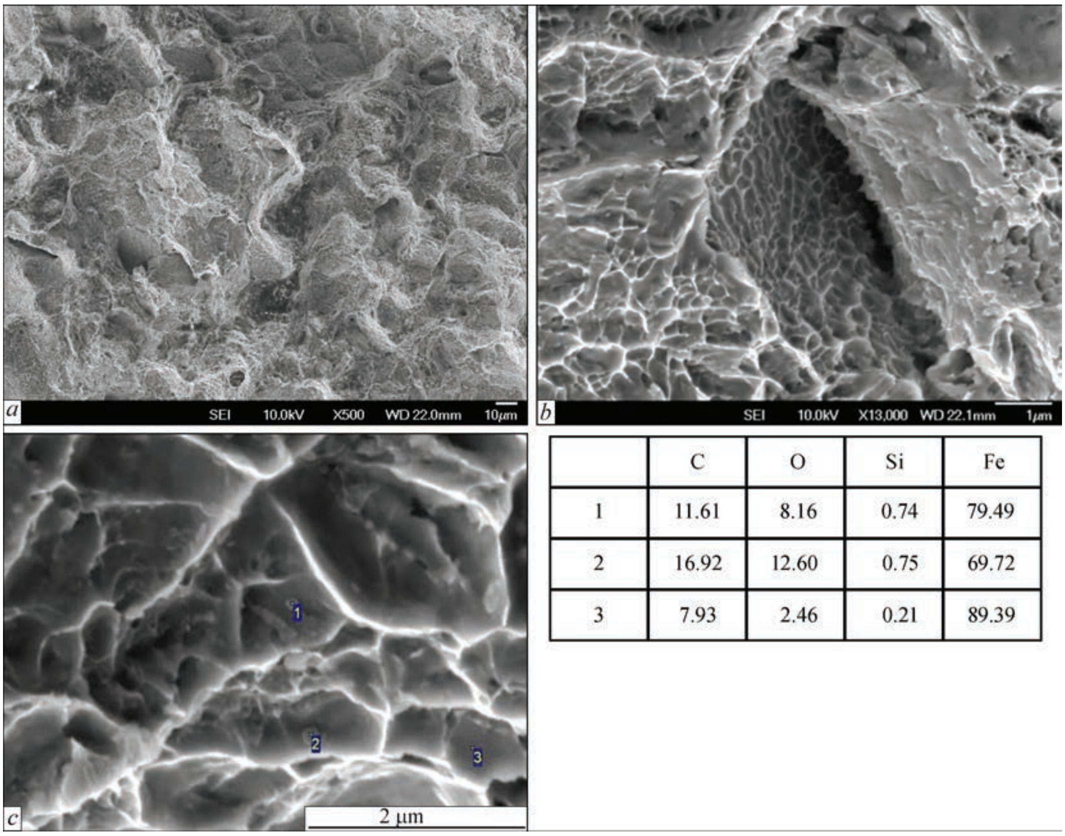

	C	O	Si	Fe
1	11.61	8.16	0.74	79.49
2	16.92	12.60	0.75	69.72
3	7.93	2.46	0.21	89.39

Figure 5. Fracture surface in the OS region (*a*, *b*), particles on facets of intragranular fracturing (*c*) and results of X-ray microanalysis of chemical composition (at.%)

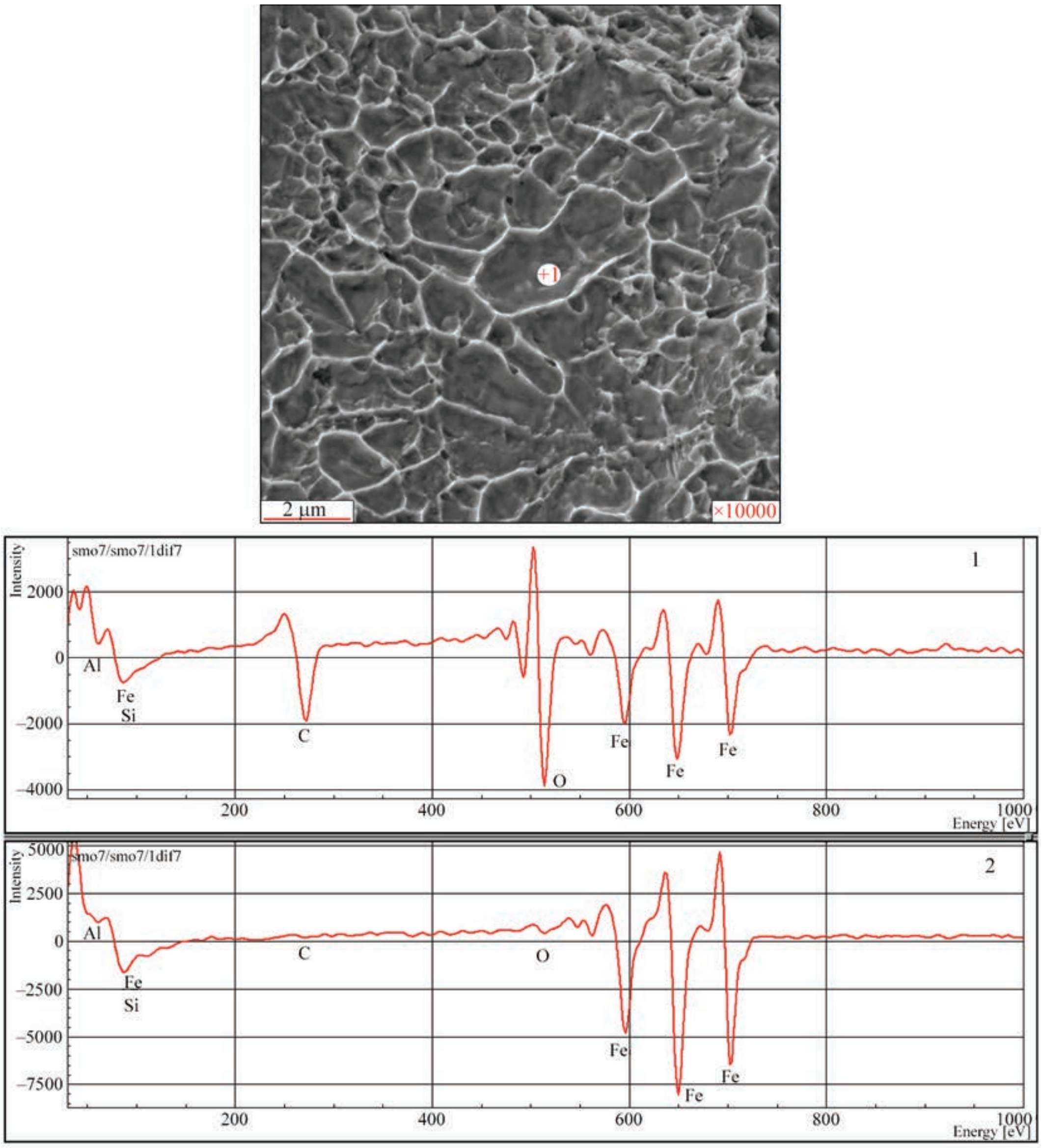

Spectrum	C	O	Fe	Si	Al	Mn	Cr	V	Ti
1	44.2	30.5	20.0	3.9	4.4.				
2	3.0	2.9	85.1	7.3	1.7				

Figure 6. Results of Auger-spectral analysis of dimples surface in the OS region (at.%): *1* — before ion etching; *2* — after ion etching

of the examination suggest that opening of metal in the OS region occurs on the oxide film, which is located on the grain boundaries. Apparently, the film is a complex, mainly, iron oxide, with some amount of aluminium oxide.

Therefore, according to the fractographic examinations, on the one hand, the nature of fracture is determined by the microstructure of rail steel, and on the other, by the presence of oxides. Within OS, the determining factor is the oxide film. In the tempering region at a smaller amount of oxide films, microstructure of metal plays a significant role, which provides some plasticity of steel unlike brittle fracturing of a heat-hardened layer.

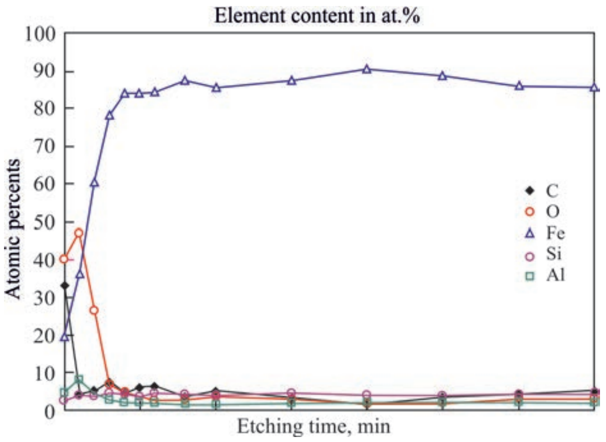

Figure 7. Distribution of elements in depth from the dimple surface in the OS region at an etching rate of 20 nm/min

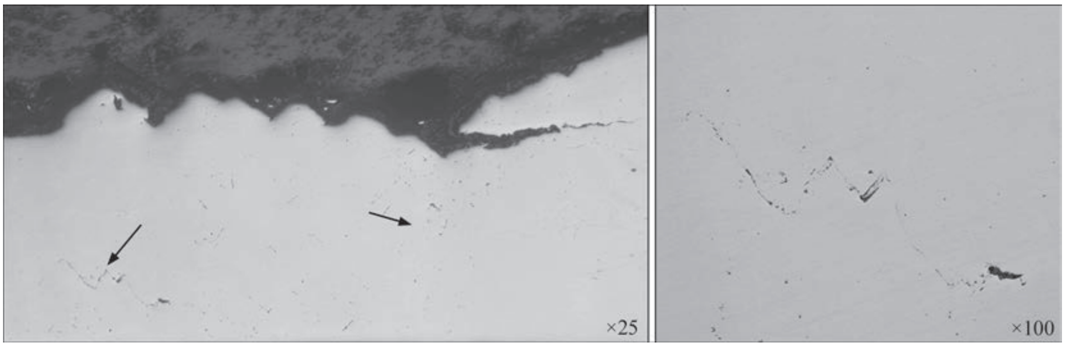

Figure 8. Nonmetallic inclusions in the rail metal adjacent to OS

In order to find the origin of oxide films, metallographic examinations of rail metal in the region adjacent to the OS were carried out. Numerous nonmetallic inclusions were found on the polished surface of the cross-section (Figure 8). According to the data of micro X-ray spectral analysis, in the metal, numerous iron oxides (Figure 9) are observed along with the inclusions of complex aluminium, silicon, calcium oxides typical to the converter rail steel. Iron oxides are located mainly on the grain boundaries. Obviously, the presence of a large number of iron oxides is associated with insufficient degree of rail steel deoxidation.

The nonuniform distribution and formation of clusters of iron oxides are caused by the features of ingot crystallization [5]. The impurities partially soluble in iron, including oxygen, are pushed into residual melt. In the places of residual melt crystallization at the structural boundaries, iron oxides are precipitated.

It is known [6] that the Fe–O system is characterized by the presence of FeO oxide (wüstite) with a melting point of 1380 °C. Between iron and wüstite, eutectics is formed at 1368 °C. FeO in the composition of oxide inclusions significantly reduces both their melting point and ductility [7]. Thus, the $FeO–Al_2O_3$ system has eutectics with a melting point of 1329 °C, the $FeO–SiO_2–Al_2O_3$ system has eutectics with a temperature of 1148 °C, the $FeO–SiO_2–CaO$ system has triple eutectics with a temperature below 1100 °C. Taking into account the level of melting points of the listed oxide systems, it is obvious that the rail steel with insufficient deoxidation level has prerequisites for the formation of oxide films. Thus, the films of iron oxide in the rails (see Figure 1, *a*, *b*) are probably formed at the stage of blooming production in the crimping shop [8]. During flash-butt welding of rails in thermodeformational conditions of joint formation, the formation of films can propagate. In this case, due to metal deformation, nonmetallic inclusions of aluminium, silicon and calcium oxides interact with iron oxides. As a result, the melting point of oxide films is decreased and the melt ductility is reduced at the ends of the parts. As a result, the OS area found on the fracture surface at a distance of 7 mm from the joint line, is much larger, OS spread to the head surface (Figure 1, *c*) [9]. In the fracture dimples, in this case, the places with numerous aluminium, silicon and calcium oxides of 1 μm were detected (Figure 10), which

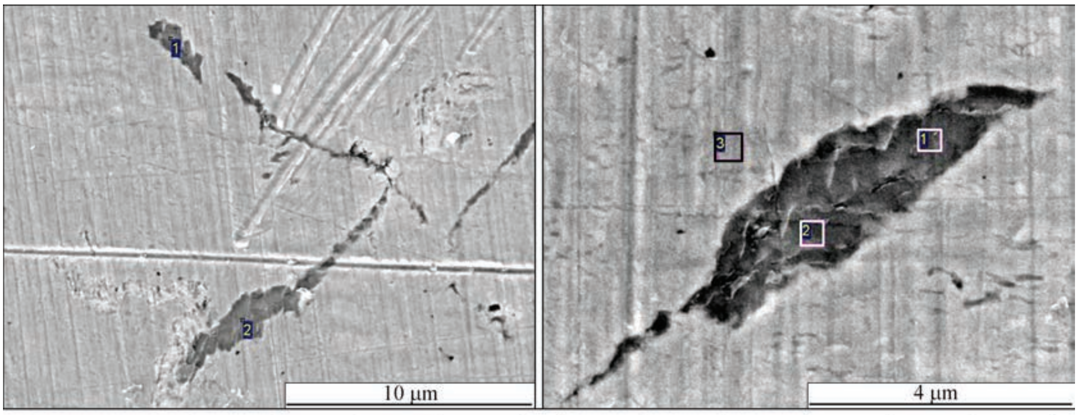

	C	O	Si	Mn	Fe
1	4.00	56.15	0.28	0.72	38.85
2	8.09	49.05	0.70	0.75	41.41

	C	O	Si	Mn	Fe
1	3.58	61.60	0.27	0.14	33.40
2	3.63	61.21	0.42	0.16	33.79
3	6.85	0.49	0.75	0.87	90.86

Figure 9. Results of micro X-ray spectral analysis of nonmetallic inclusions (at.%) in the rail metal adjacent to OS

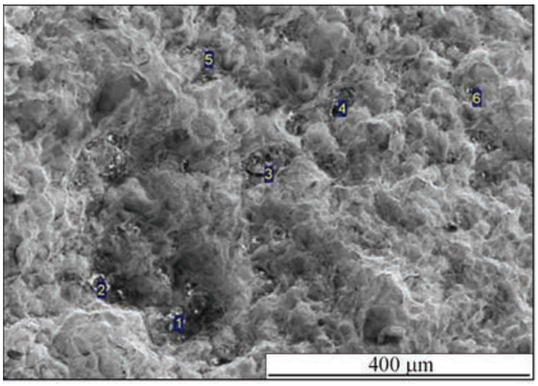

	C	O	Mg	Al	Si	S	Ca	Fe
1	34.38	7.29		0.68	3.60		4.58	45.64
2	46.57	29.02		1.47	4.41	1.53		2.40
3	24.0	23.21		1.49	3.27		0.74	47.29
4	49.32	33.95	0.23	1.87	6.48	0.30	0.79	6.03
5	55.94	27.26	0.45	2.35	6.54		1.18	5.57
6	26.55	53.09	0.36	1.25	2.61	2.41	10.22	1.86

a

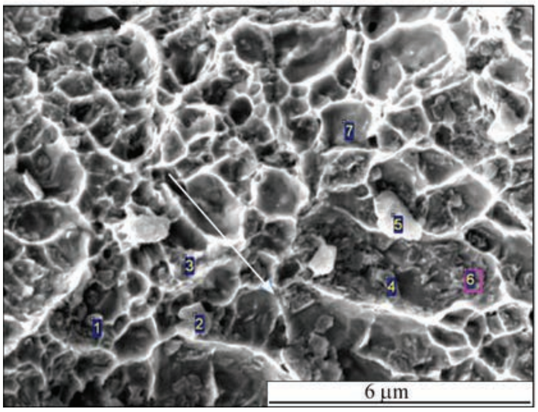

	C	O	Al	Si	S	Ca	Fe
1	16.48	3.78	0	1.02			78.62
2	28.58	19.54	0	1.03	1.46	2.14	46.66
3	16.05	9.34	0.67	1.48			72.46
4	18.36	24.75	3.20	**5.00**			48.69
5	18.83	52.32	**5.01**	**15.22**			4.75
6	17.46	4.58	0.31	0.57			77.07
7	3.52	0.17	0	0.40			95.92

b

Figure 10. Fracture surface and X-ray microanalysis (at.%) of chemical heterogeneity in the OS region during fracturing of a butt joint at a distance of 7 mm from the joint line

confirms the participation of these oxides in the formation of oxide film.

It is worth noting the difference of OS from the known "matte spots" [9] observed on the fracture surface of the joints of KF76 rails. "Matte spots" is the result of interaction in the near-contact layer of silicon-containing oxide inclusions with the surface-active manganese in iron and a subsequent formation of silicate films [10]. It is known [11], that oxide films negatively affect the properties of steel. Thus, in [12] a decrease in the relative reduction in area of the rail steel metal with insufficient deoxidation is noted. The presence of OS on the fracture surface during static bending tests is the evidence of insufficient deoxidation degree and the factor of reduced steel quality.

CONCLUSIONS

1. According to the data of micro X-ray spectral analysis of the fracture surface of the welded butt joints of K76F rails, along with the inclusions of complex oxides of aluminium, silicon and calcium typical for converter rail steel, in the metal, numerous iron oxides are observed, which are located mainly on the grain boundaries. The presence of a large number of iron oxides is associated with insufficient degree of rail steel deoxidation.

2. Fracturing of K76F rails on iron oxide films during static bending tests is a sign of insufficient degree of steel deoxidation and a probable cause of reduced service characteristics of rails and their welded butt joints.

REFERENCES

1. Botshtein, V. A., Rudyuk, A. S., Chichkarev, E.A. et al. (2013) Mastering of converter rail steel production at PJSC MK Azovstal. *Metall i Lityo Ukrainy,* 241(**6**), 34–37 [in Ukrainian].
2. (2016) TU U 27.1-40075815-002:2016: *Rails are new welded for railways*.
3. Kuchuk-Yatsenko, S.I., Didkovsky, O.V., Bogorsky, M.V. et al. (2002) *Method of flash-butt welding*. Pat. 46820 Ukraine, 6 B23K11/04, C2. Publ. 06/17/2002 [in Ukrainian].
4. Kuchuk-Yatsenko, S.I., Didkovsky, O.V., Antipin, Ye.V. et al. (2016) Flash-butt welding of high-strength rails, mining – informatics. *Automation and Electrical Eng.*, 528(**4**), 40–48.
5. Samoilovich, Yu.A. (1983) *System analysis of ingot crystallization*. Kyiv, Naukova Dumka [in Russian].
6. Barabash, O.M., Koval, Yu.N. (1986) *Crystal structure of metals and alloys*: Reference. Kyiv, Naukova Dumka [in Russian].
7. (1985) *Atlas of slags*: Reference. Ed. by I.S. Kulikova. Moscow, Metallurgiya [in Russian].
8. Levchenko, N.V. (2006) Variation of nonmetallic inclusions during rail production. *Metallurgical and Mining Industry*, **2**, 63–65.
9. Kuchuk-Yatsenko, S.I., Shvets, V.I., Didkovsky, A.V., Antipin, E.V. (2016) Effect of non-metallic inclusions of rail steel on welded joint formation. *The Paton Welding J.*, **5–6**, 24–28. DOI: https://doi.org/10.15407/tpwj2016.06.04
10. Shvets, V.I., Ziakhor, I.V., Kapitanchuk, L.M. (2023) Features of formation and transformation of oxides in flash-butt welding of K76F rails. *The Paton Welding J.*, **7**, 16–24. DOI: https://doi.org/10.37434/tpwj2023.07.02

11. Gubenko, S.I. (2015) *Nonmetallic inclusions and strength of steels*. Palmarium Academic Publ.
12. Trotsan, A.I., Kaverinsky, V.V., Koshule, I.M., Nosochenko, A.O. (2013) On the factors influencing the quality of rail steel and rails. *Metall i Litiyo Ukrainy,* 241(**6**), 9–14.

ORCID

V.I. Shvets: 0000-0003-4653-7453,
I.V. Ziakhor: 0000-0001-7780-0688,
O.V. Didkovskyi: 0000-0001-5268-5599,
E.V. Antipin: 0000-0003-3297-5382

CONFLICT OF INTEREST

The Authors declare no conflict of interest

CORRESPONDING AUTHOR

I.V. Ziakhor
E.O. Paton Electric Welding Institute of the NASU
11 Kazymyr Malevych Str., 03150, Kyiv, Ukraine.
E-mail: zyakhor2@ukr.net

SUGGESTED CITATION

V.I. Shvets, I.V. Ziakhor, L.M. Kapitanchuk, O.V. Didkovskyi, E.V. Antipin (2024) Peculiarities of fracture of welded joints of railway rails of oxygen-converter K76F steel. *The Paton Welding J.*, **5**, 3–10.

JOURNAL HOME PAGE

https://patonpublishinghouse.com/eng/journals/tpwj

Received: 07.03.2024
Received in revised form: 09.04.2024
Accepted: 27.05.2024